Downscaling and Projections of Spatiotemporal Variations of Precipitation of Iraq under RCP Scenarios

Saleem A. Salman[1], Shamsuddin Shahid[1], Kamal Ahmed[2*], Ahmad Sharafati[3], Ghaith Falah Ziarh[1], Tarmizi Ismail[1], Eun-Sang Chung[4], and Xiao-Jun Wang[5]

[1]Department of Hydraulics & Hydrology, Faculty of Civil Engineering, Universiti Teknologi Malaysia, Johor Bahru, Malaysia
E-mail: assaleem2@live.utm.my; sshahid@utm.my; tarmiziismail@utm.my; eng.ghaith.ziarh@gmail.com

[2]Department of Water Resources Management, Lasbela University of Agriculture, Water, and Marine Sciences, Lasbela, Balochistan, Pakistan. E-mail: kamal_brc@hotmail.com

[3]Department of Civil Engineering, Science and Research Branch, Islamic Azad University, Tehran, Iran. Email: asharafati@gmail.com

[4]Faculty of Civil Engineering, Seoul National University of Science and Technology, 01811, Seoul, Republic of Korea, Phone: +82 2 9709017; Fax: +82 2 9480043; E-mail: eschung@seoultech.ac.kr

[5]State Key Laboratory of Hydrology-Water Resources and Hydraulic Engineering, Nanjing Hydraulic Research Institute, Nanjing 210029, R.P. China. E-mail: xjwang@nhri.cn

Downscaling and Projections of Spatiotemporal Variations of Precipitation of Iraq under RCP Scenarios

Abstract

The spatiotemporal changes in precipitation pattern can have crucial implications in arid region due to its frail environment. An analysis is conducted to estimate the probable spatiotemporal alteration of annual and seasonal precipitation of Iraq through statistical downscaling of global climate model (GCM) simulations for different representative concentration pathways (RCP) scenarios. Symmetrical uncertainty (SU) and compromising programming are used for the ranking and selection of GCMs. Model Output Statistics (MOS) downscaling models are implemented using support vector machine with selected GCM variables as predictors and global precipitation climatology Centre (GPCC) precipitation as predictand. An intelligence merging approach based on Random Forest is developed to construct multi-model ensemble (MME) projection of precipitation. The results indicate more uncertain in precipitation increase in the earlier period (2010-2039) compared to the later period (2070-2099) for all scenarios. The projected seasonal precipitation changes indicate an increase in almost all months (Jan-Dec) during 2010-2039 with a higher increase in winter and almost no change in summer. The spatial pattern of the changes reveals the highest decrease in precipitation in the north and northwest by -58 to -94 mm, while an increase in the middle, northeast and southeast by 6 to 18 mm for different RCPs. The results of the study have potential to be utilized for strategizing policies for building climate resiliency in Iraq.

***Keywords*:** Global climate models, precipitation downscaling, support vector machine, random forest, arid region.

1. Introduction

Interpretation of general circulation model (GCM) runs for future periods revealed a continuous rise of Earth's surface temperature and thus an increase in evaporation and atmospheric water contents, and alteration of precipitation and hydrological regimes (Ouyang et al. 2015; Shahid et al. 2016; Wang et al. 2016). Such changes are projected much higher for arid regions, particularly in the west Asia (IPCC 2007; Pour et al. 2020; Salman et al. 2018a). Regions dominated by arid climate are highly susceptible to any minor alterations of climate regimes due to their frail ecosystems (Ahmed et al. 2019f; Salman et al. 2017; Sarr 2012). Besides, scarce precipitation makes such regions highly prone to hydrological extremes such as heavy rainfall-driven floods and severe droughts (Buytaert et al. 2012; Houmsi et al. 2019; Salman et al. 2018c; Wu et al. 2016). A little change in precipitation pattern causes a significant rise in precipitation extremes (Chiew et al. 2009; Groisman et al. 1999; Khan et al. 2019; Nashwan and Shahid 2018; Nashwan et al. 2019; Pour et al. 2014; Shahid 2011; Shiru et al. 2019b). Hence, a large changes in climate may severely affect the western part of Asia with various climate-related disasters (Pour et al. 2018; Salman et al. 2017; Salman et al. 2018c).

GCMs, generally used for climate modeling often provide unrealistic climate projections (Akhter et al. 2019; Onyutha et al. 2016; Xu et al. 2019). The appropriate GCMs is usually selected according to their performance in modeling the present climate to project the future climate variables of a region (Lutz et al. 2016; McSweeney et al. 2015; Salman et al. 2018a; Shiru et al. 2019a). Generally, multiple statistical indices are employed to decide GCM capability in modeling the existing climate of the area of interest (Ahmed et al. 2019c; Noor et al. 2019a). However, such metrics often provide conflicting results and make GCM selection intrigue (Ahmed et al. 2019e). Hence, the necessity of sophisticated approaches is evident to select a reliable GCM set for climate change projections. The use of machine learning (ML) techniques in GCM performance assessment has significantly increased in recent years (Ahmed et al. 2019d; Khan et al. 2018; Pour et al. 2018; Shiru et al. 2019a). The previous studies reported that symmetrical uncertainty (SU) (Press et al. 1996) is the most suitable for GCM selection among the all ML methods.

High-resolution climate projections are needed for majority of impact assessment studies (Fallmann et al. 2017; Gebrechorkos et al. 2019; Navarro-Racines et al. 2020). Hence, GCMs outputs are commonly downscaled to higher resolution mostly by statistical downscaling (SD) (Ahmed et al. 2015; Alamgir et al. 2020; Sa'adi et al. 2017). The perfect prognosis (PP) and model output statistics (MOS) are two major types of SD methods (Vandal et al. 2019; Xu et al. 2020). The MOS is more efficient in bias-correction than the PP method, and it much widely used in recent years in downscaling GCM outputs (Nashwan et al. 2020; Noor et al. 2019b; Turco et al. 2017). The regression MOS is the recent development of climate downscaling, where a climate variable is downscaled using regression model developed based on the in-situ and GCM climate variables (Ahmed et al. 2019d; Eden et al. 2012; Eden et al. 2014; Sa'adi et al. 2017; Shirvani and Landman 2016). For example, precipitation at a location is downscaled through the development of a regression model with in-situ precipitation as predictand and related GCM variables as predictors. Such multi-variable bias correction method improves the performance of downscaling and provides reliable projections of climate (Ahmed et al. 2019a; Moghim and Bras 2017; Pour et al. 2018). The performance of multi-variable bias correction depends on the method used for regression model development. The non-linear association between in-situ and GCM climate variables urges the necessity of sophisticated methods for the implementation of such model.

A procedure for methodic selection of GCMs and downscaling of their simulations using a multi-variable bias correction approach is proposed in this study to project the spatiotemporal changes in precipitation of Iraq. ML algorithms are used for several purposes such as selection of GCMs, development of downscaling model and generation of GCMs ensemble mean projections. The novel procedure presented in this article can be replicated for trustworthy climate projections in any region of interest.

2. Materials and Methods

2.1 Geography and Climate of Iraq

Iraq, situated in southwest Asia and bounded by geographical coordinates of (38°45′E,29°15N) and (48°45′E,38°15′N), covers an area of 438,320 km^2 (Salman et al. 2020; Yaseen et al. 2018). The climate in most of the country is subtropical desert (BWh) (Fig 1-a) (Salman et al. 2020).

Besides, the climate in two small strips in the north are considered as subtropical steppe (BSh) and subtropical (Csa) according to Köppen's definition. The three climate zones are defined as Zone-I, II and III, respectively, in this study. Precipitation in Iraq varies widely among the three climate zones, nearly 63 mm in the southwest of Zone-I to 900 mm and above in Zone-III (Fig 1b).

Iraq's climate is divided into two main seasons, summer (Jun–Sept), and winter (Nov–Mar). Spring and Autumn are two transition seasons between these two major seasons. The country experiences nearly 90% precipitation in winter (Fig 1c). Therefore, summer is usually extremely dry (Al-Ansari 2013; Salman et al. 2019; Salman et al. 2017). Temperature drops near to freezing point especially in Zone-III during winter while it often rises above 45°C in some summer days, particularly in the south of Zone-I.

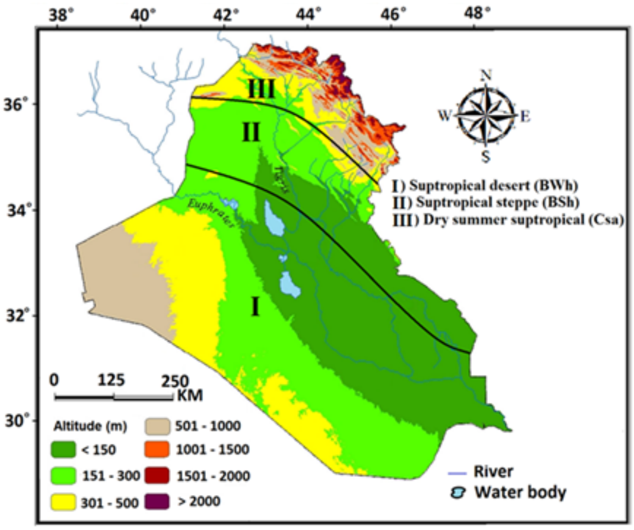

(a)

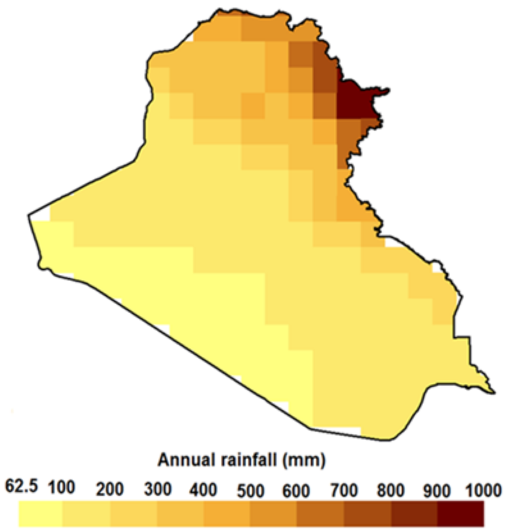

(b)

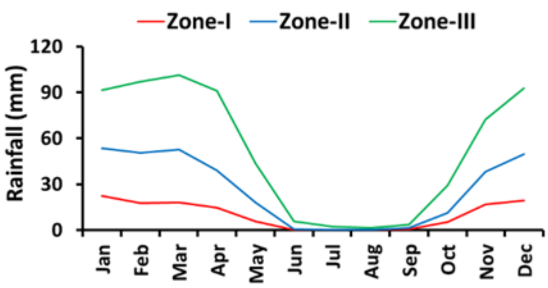

(c)

Fig 1. (a) Climate zones over the topographic map; (b) spatial precipitation patterns; (c) seasonal precipitation variations in Iraq.

2.2 Data and Sources

GPCC precipitation extracted from the data portal of www.esrl.noaa.gov/psd/data/gridded/data.gpcc.html is utilized as a reference dataset for selection of GCMs, and downscaling and projection of precipitation of Iraq. GPCC precipitation has been proved as most efficient in reproducing in-situ precipitation of Iraq by Salman et al. (2018b).

Several GCMs are available in the coupled model intercomparison project (CMIP5). The GCMs having simulations for all the RCPs are considered for their performance assessment (Table 1). To downscale the precipitation, the GCM predictors namely, air temperature, sea level pressure, relative and specific humidity, eastward and northward wind and geopotential height at four pressure levels namely, 925,850,700,600 and 500 are used. Those data are obtained from the website of https://cds.climate.copernicus.eu. The GCMs variables are re-gridded into 2°×2° resolution for selection of GCMs. The 2° resolution is selected based on the mean resolution of the considered GCMs.

Table 1. The global climate models considered in the study

No	GCM	Institute	Resolution (Lon x Lat)
1	BCC-CSM1-1	Beijing Climate Center, China	2.8° × 2.8°
2	CanESM2	Canadian Centre for Climate Modelling and Analysis, Canada	2.8° × 2.8°
3	GISS-E2-H	NASA Goddard Institute for Space Studies, USA	2.5° × 2.5°
4	HadGEM2-ES	Met Office Hadley Centre, UK	1.87° × 1.25°
5	MIROC5	Agency for Marine-Earth Science and Technology, Japan	1.4° × 1.4°
6	MIROC-ESM		2.8° × 2.8°
7	MIROC-ESM-CHEM		2.8° × 2.8°
8	NorESM1-M	Norwegian Meteorological Institute, Norway	2.5° × 1.9°
9	NorESM1-ME		2.5° × 1.9°
10	MPI-ESM-LR	Max Planck Institute for Meteorology, Germany	1.87° × 1.86°
11	MPI-ESM-MR		1.87° × 1.86°
12	BCC-CSM1.1(m)	Beijing Climate Center, China	2.8° × 2.8°
13	CNRM-CM5	Centre National de Recherches Météorologiques, France	1.4° × 1.4°
14	HadGEM2-AO	National Institute of Meteorological Research, Korea	1.87° × 1.25°
15	CCSM4	National Center for Atmospheric Research, USA	1.25° × 0.94°
16	CSIRO-Mk3.6.0	Commonwealth Scientific and Industrial Research Organization, Australia	1.86° × 1.87°
17	INMCM4.0	Institute of Numerical Mathematics, Russia	2.0° × 1.5°
18	CMCC-CM	Centro Euro-Mediterraneo sui Cambiamenti Climatici, Italy	0.75° × 0.75°
19	GFDL-CM3	Geophysical Fluid Dynamics Laboratory, USA	2.5° × 2.0°

20	CMCC-CMS	Centro Euro-Mediterraneo sui Cambiamenti Climatici, Italy	3.75° × 3.71°

3. Methodology

3.1 Procedures

The following steps are used for GCM selection, statistical downscaling and precipitation projections:

i. GCM precipitations are interpolated into the considered resolution of 2°×2°. The GPCC precipitation is also upscaled to the same resolution for comparison.

ii. SU is used to evaluate the similarity between the annual precipitation simulated by GCM and produced by GPCC over the grid points of Iraq.

iii. Compromise programming index (CPI) is used to assimilate ranking of all the grid points over Iraq to estimate the overall ranking of GCMs for the country.

iv. All the selected GCM predictors are interpolated to the resolution of GPCC (0.5°×0.5°).

v. Stepwise regression is used to choose the GCM predictors from multiple levels for precipitation prediction at all the GPCC grid points of Iraq. Predictors are selected for each month separately to capture seasonal variability in precipitation.

vi. Selected GCM predictors (Fig 2) are used as input in a support vector machine (SVM) where the GPCC precipitation is considered as output to develop MOS models.

vii. The downscaling models are used to project the precipitation for four RCPs.

viii. RF regression is utilized to calculate the multi-model ensemble (MME) mean of projected precipitation.

ix. The MME mean precipitation for three future periods (2010 – 2039, 2040 – 2069, and 2070 – 2099) are utilized to assess the future precipitation changes.

Methods are elaborated in the following sections.

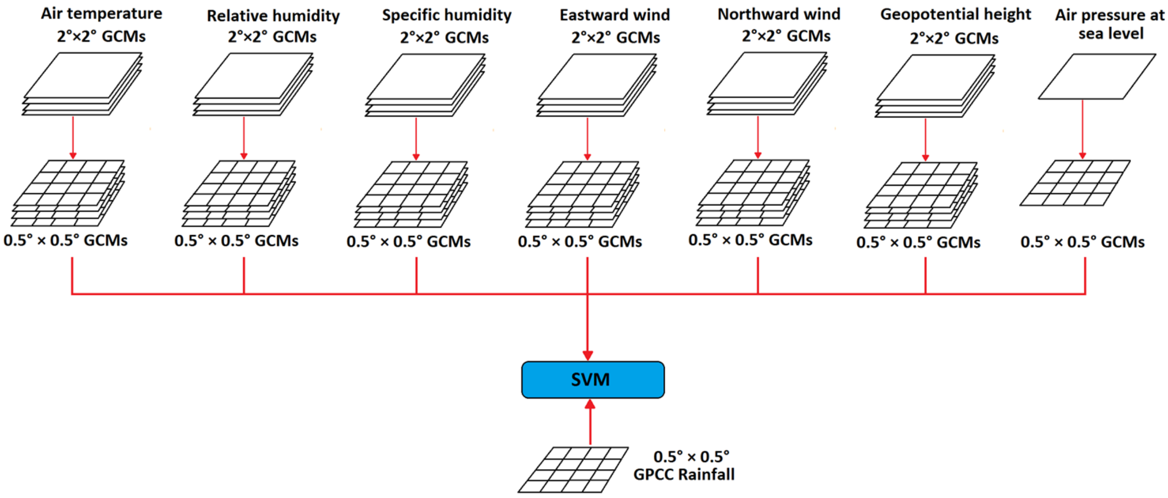

Fig 2. The multi-variable model output statistics (MOS) downscaling of precipitation

3.2 Symmetrical Uncertainty (SU)

The SU assesses similarity between the GCM and GPCC precipitation using the concept of information entropy. If GCM precipitation is similar to GPCC precipitation, the information gain (IG) is high and vice-versa. The higher precipitation depths usually provide larger IG values. SU is used to overcome the IG's shortcoming of inclination of higher values. The SU between GCM and CPCC precipitation (X_i and X_j respectively) can be estimated from their entropies ($H(X_i)$ and $H(X_j)$) as

$$SU(X_i, X_j) = 2\left[\frac{IG(X_i|X_j)}{H(X_i)+H(X_j)}\right] \quad (1)$$

A SU value near to unity means the high similarity and vice-versa (Shreem et al. 2016).

3.3 Compromise programming index (CPI)

The SU ranks the GCMs according to their performance at individual grid locations. The CPI is used to assimilate the ranking of all the grid points (18 grid points to cover the country). The CPI is estimated as

$$CPI = \left[\sum_{i=1}^{n} |x_i^1 - x_i^*|^p\right]^{1/p} \quad (2)$$

where; x_i^1 is the rank of a GCM, x_i^* is the ideal rank (considered 1 in this study) and p is a parameter. To provide a linear equation, p is considered to 1. A GCM with highest CPI value offers the best performance. The GCMs with ranks below or equal to 3 are considered to estimate CPI. Others are assigned a zero CPI.

3.4 Support vector machine (SVM)

SVM regression is used to develop the MOS model for downscaling the GCMs. SMV mathematically express the connection of GPCC precipitation, (y) with GCM predictors, (x_i) as,

$$y = f(x_i) = w\phi(x_i) + b \quad (3)$$

where w and b represent weight vector and error, respectively; ϕ is the kernel function. In SVM, the parameters (w, b) are minimized to derive the optimum relationship. The statistical software R package *e1071* is used for model development. The model is trained for the period of 1961 to 1993 and tested for 1994–2005. A cross-validation approach is employed to optimize the hyperparameters of the SVM model.

3.5 An ensemble using Random Forest (RF) regression

A non-linear regression model developed by RF is employed to generate the MME mean of GCM precipitation (Ahmed et al. 2019b; Ahmed et al. 2019d; Sa'adi et al. 2017; Salman et al. 2018a). The precipitation of selected GCMs are considered as input and the GPCC precipitation as output for development of RF model at each grid. The training and testing periods for the RF model are similar to those considered for the SVM model. The developed RF model is used to produce the MME mean of precipitation projections of selected GCMs. The MME mean precipitation is finally used for evaluation of future changes in precipitation in comparison to historical precipitation (1971 – 2000).

4. Results and discussion

4.1 GCM ranking

The spatial distribution of the GCMs for the top three ranks provided by SU over the 18 grid points of Iraq is shown in Fig 3. The GCMs are represented by different colors in the maps. The figure shows that the NorESM1-M provides the best precipitation simulation in majority of grid locations. The CSIRO-Mk3-6-0 has better accuracy in the east and BCC-CSM1.1(m) at a few southeast grids. The BCC-CSM1-1 and CSIRO-Mk3-6-0 found as the second best models in the middle and west respectively. Those GCMs are also found to be the third best model in a major part of Iraq.

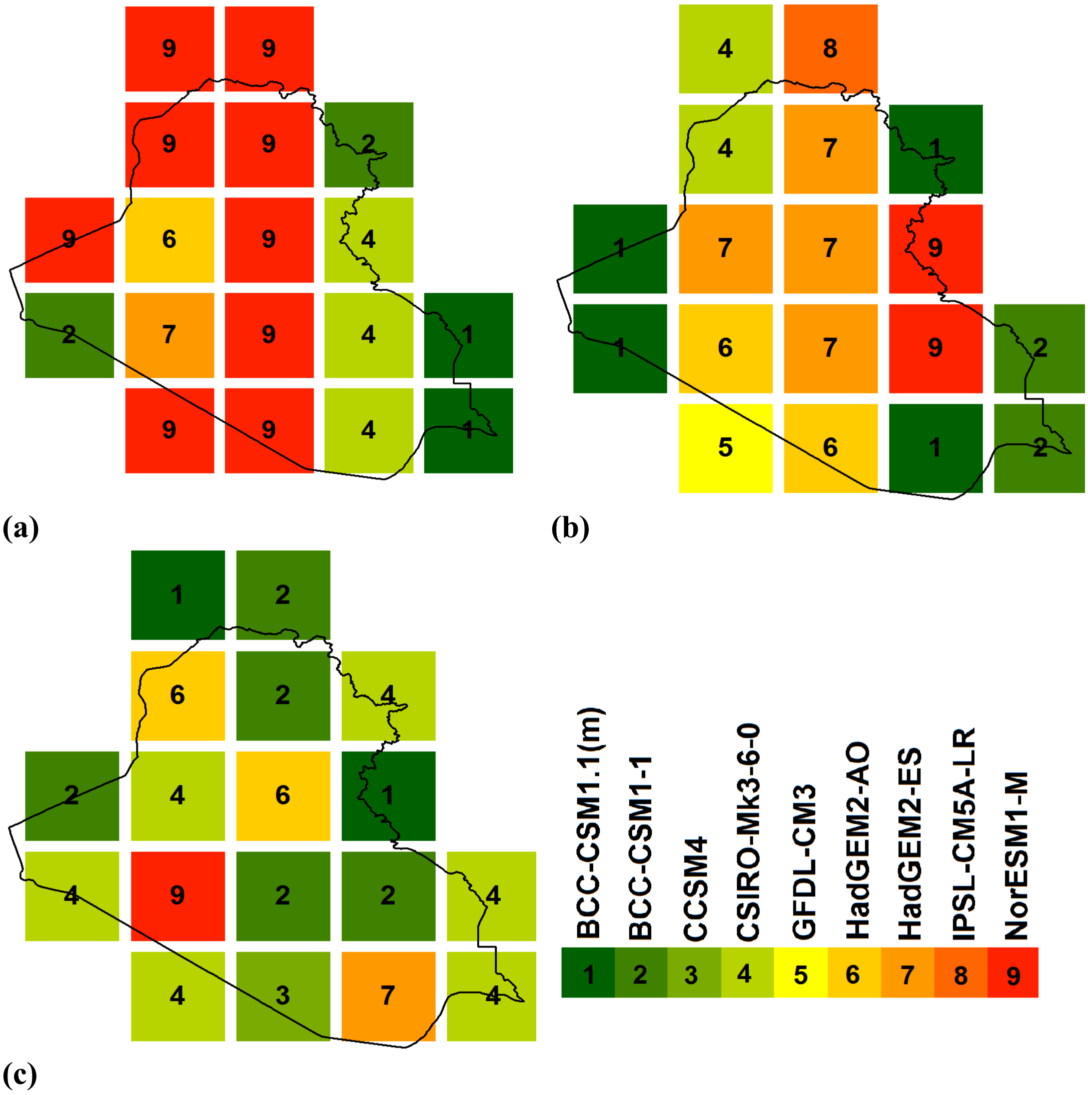

Fig 3. The GCMs ranked (a) first; (b) second; and (c) third by SU in modelling precipitation at different gird locations of Iraq

The CPI estimated for each GCMs by aggregating their ranking at different grid points is given in Table 2. Nine GCMs (NorESM1-M, CSIRO-Mk3-6-0, BCC-CSM1.1(m), BCC-CSM1-1, HadGEM2-ES, HadGEM2-AO, GFDL-CM3, IPSL-CM5A-LR, CCSM4) are found to obtain a CPI more than zero, and therefore, those GCMs are initially selected.

Table 2. Compromise programming index estimated for different GCMs for Iraq

GCM	CPI
NorESM1-M	10.33

CSIRO-Mk3-6-0	5.98
BCC-CSM1.1(m)	4.66
BCC-CSM1-1	4.65
HadGEM2-ES	3.33
HadGEM2-AO	2.66
GFDL-CM3	0.5
IPSL-CM5A-LR	0.5
CCSM4	0.33
CESM1-CAM5	0
FIO-ESM	0
GFDL-ESM2G	0
GFDL-ESM2M	0
GISS-E2-H	0
GISS-E2-R	0
IPSL-CM5A-MR	0
MIROC5	0
MIROC-ESM	0
MIROC-ESM-CHEM	0
MRI-CGCM3	0

For consistency in climate change projection, it is suggested that GCMs should able to simulate both precipitation and temperature reliably. Among the top GCM given in Table 2, only two GCMs namely HadGEM2-ES and HadGEM2-AO are found common with top temperature GCMs selected for Iraq in the previous study conducted by Salman et al. (2018a). Therefore, those two GCMs are finally downscaled and used for precipitation projections.

4.2 Downscaling of GCMs precipitation

The selected GCMs are downscaled based on GPCC precipitation at a resolution of $0.5^{o}\times0.5^{o}$. The efficiency of downscaling models is visually assessed using the scatter plots of areal average annual and seasonal (summer and winter) GPCC and downscaled precipitation (Fig 4). The results obtained by each GCM demonstrate a good agreement with the monthly GPCC precipitation. Downscaling precipitation is always a difficult task. Unlike temperature downscaling, it is never possible to get a perfect match between observed and downscaled precipitation. This issue is more crucial, especially in the arid regions (Nashwan et al. 2020). Higher values are always underestimated by downscaling model for arid region as those phenomena are very erratic and rare in the arid regions (Ahmed et al. 2019d). This study also shows similar results. The higher values are underestimated for annual and both seasons, while lower values are overestimated, particularly for winter. However, the under- or over-estimations are not very high. Therefore, its accuracy of precipitation downscaling models is considered acceptable.

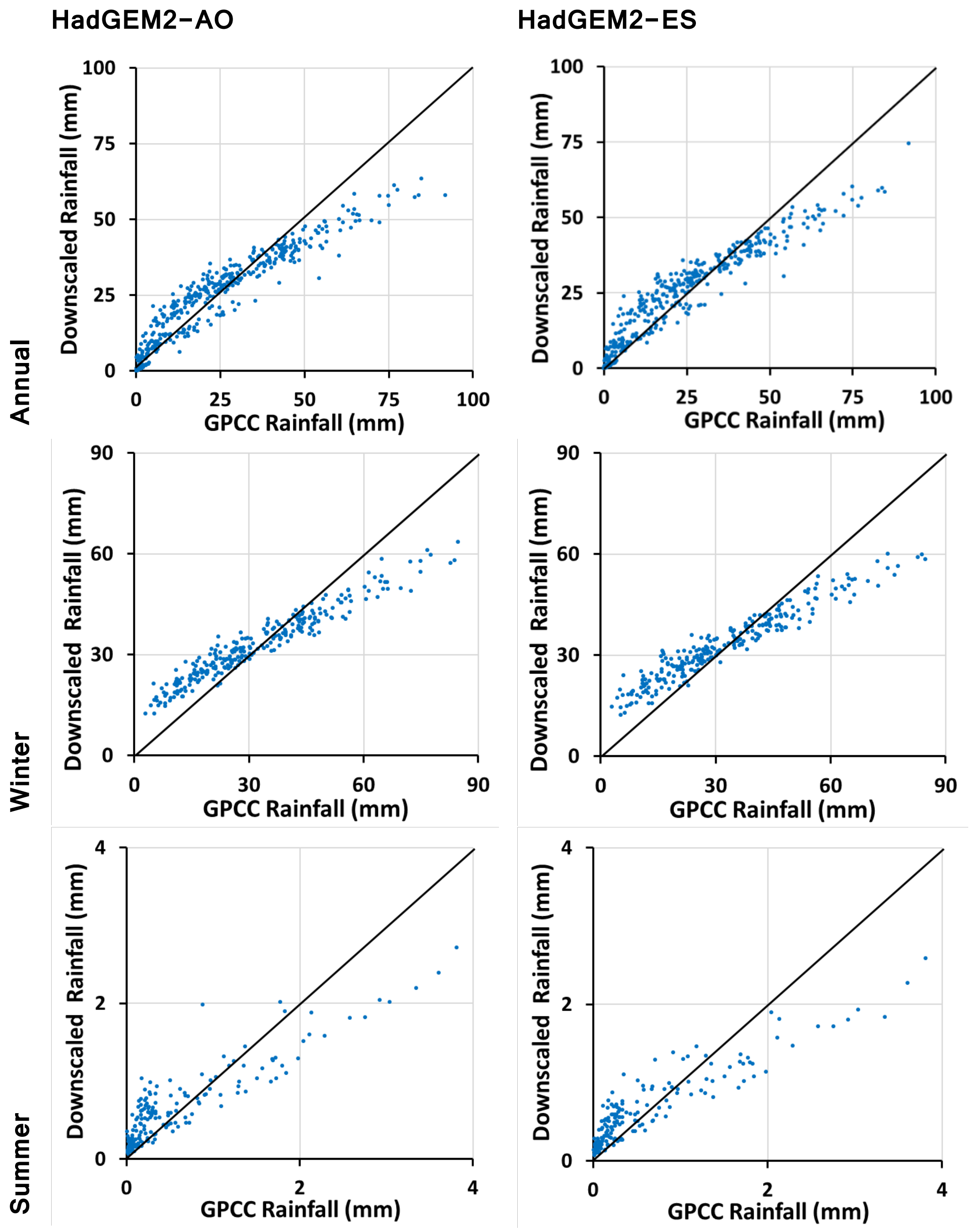

Fig Error! No text of specified style in document.. Comparison of the GPCC and downscaled GCM monthly average of annual; winter and summer precipitation (upper) to (lower)

4.3 Multi-model ensemble mean precipitation

To assess the RF performance in generation of ensemble mean, the agreements between the MME mean and the GPCC precipitation averaged for entire Iraq for both annual and seasonal scales are shown in Fig 5. The data points in the plots are aligned very close to the diagonal line, which sugests adequate competence of RF model in generating ensemble mean precipitation.

.

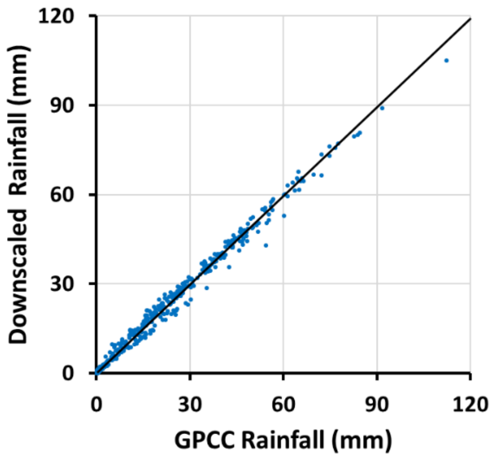

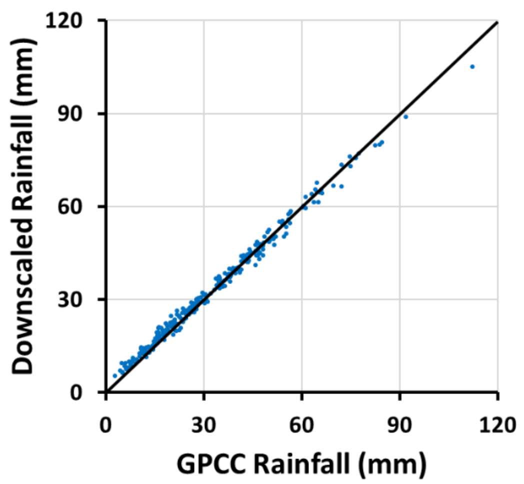

(a) **(b)**

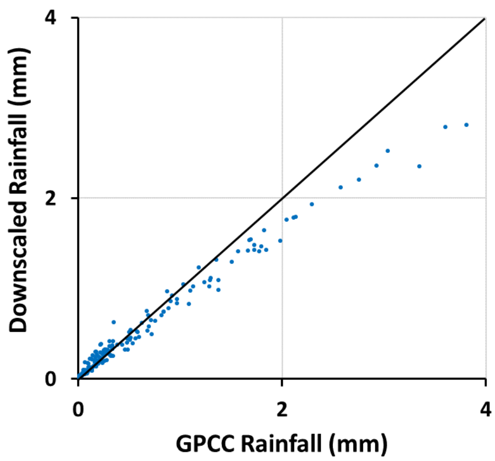

(c)

Fig 5. Comparison of GPCC and downscaled multi-model ensemble mean of （a） annual; （b） winter; and （c） summer precipitation

4.4 Projection of annual precipitation

Fig 6 demonstrates the shift in annual precipitation of Iraq for three future periods and four RCPs. The UB (blue horizontal line) in the figure represents the upper bound of precipitation change at 95% confidence level, ESM (red) refers to MME mean, and LB refers to lower bound of 95% confidence level. The MME precipitation is found closer to LB compared to UB, which indicates higher uncertainty in projection of larger raise in precipitation. A higher augmentation of precipitation is projected in the earlier period (2010-2039) compared to the last period (2070-2099) for all scenarios. Overall, the preceipitatin is projected to increase more in Zone-I compared to other zones.

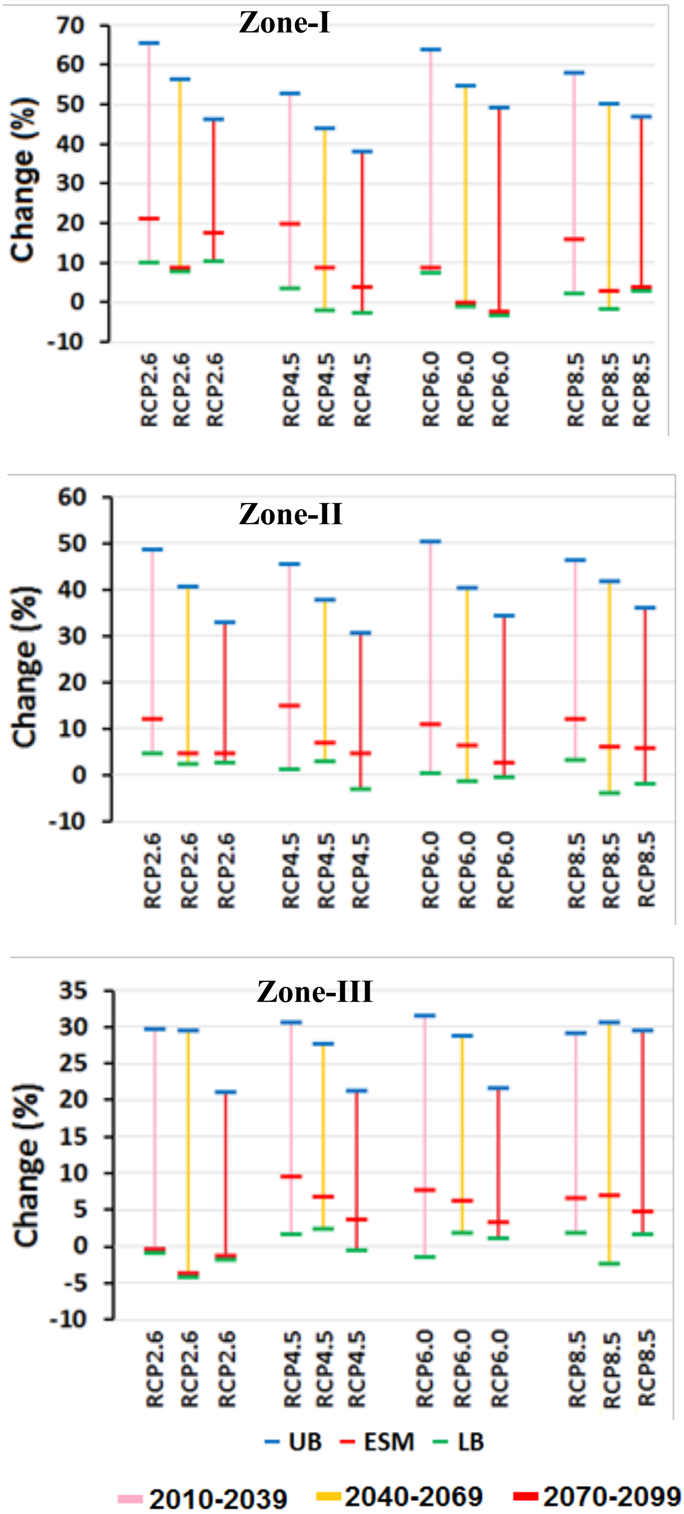

Fig 6. Changes in annual precipitation (%) in three future periods, 2010-2039 (pink), 2040-

2069 (yellow) and 2070-2099 (red) for four RCPs

4.5 Seasonal changes in precipitation

The monthly precipitation changes in different climate zones for different RCPs and three future periods are shown in Figs. 7 to 9. An increase in precipitation in almost all months is noticed during 2010-2039 (Fig. 7). A higher increase is projected for winter months, while almost no change during summer. More or less similar results are observed for 2040-2069 (Figure 8) and 2070-2099 (Figure 9). Winter precipitation is found to increase mode while almost no change in summer precipitation.

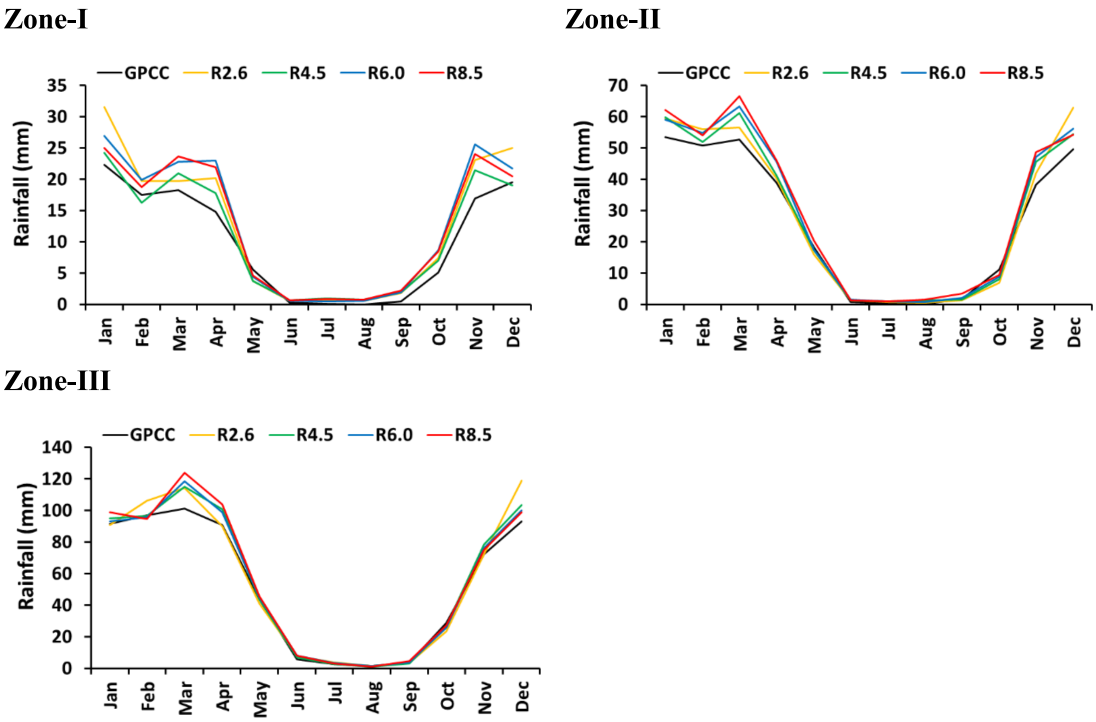

Fig 7. Changes in seasonal precipitation in three climate zones during 2010–2039 in comparison of 1961-1990 for different RCPs.

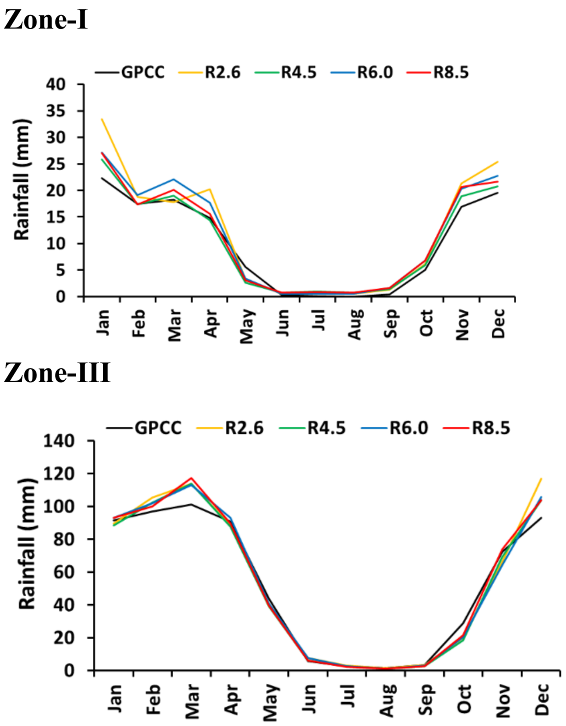

Fig 8. Changes in seasonal precipitation in three climate zones during 2040–2069 in comparison of 1961-1990 for different RCPs.

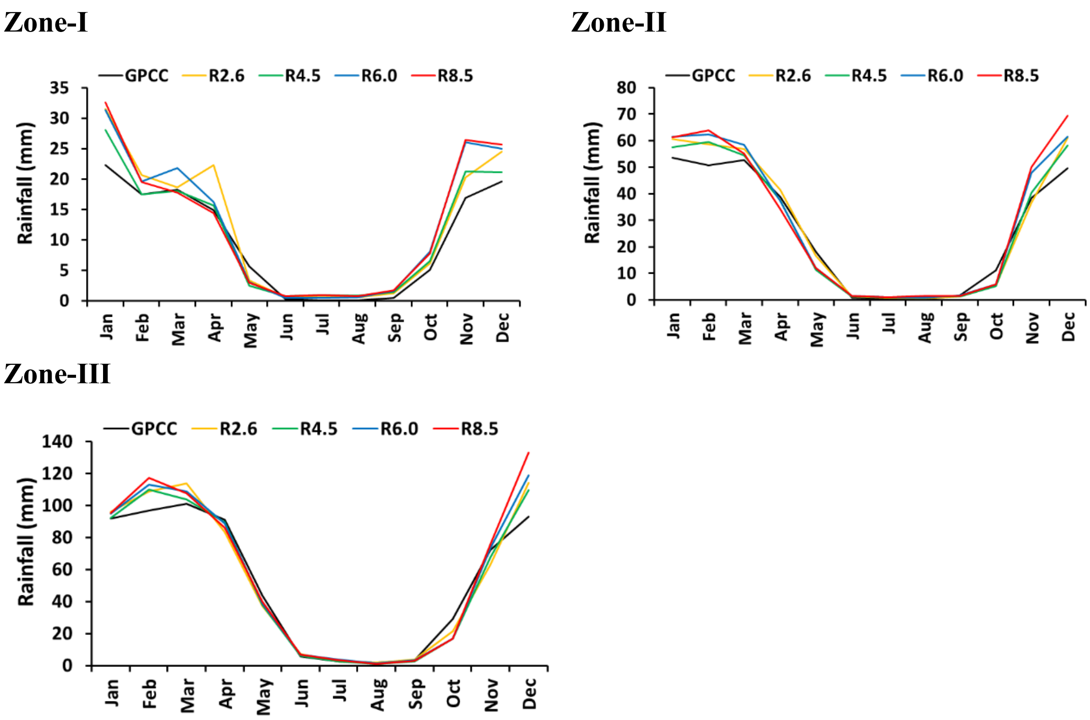

Fig 9. Changes in seasonal precipitation in three climate zones during 2070–2099 in comparison of 1961-1990 for different RCPs.

4.6 Geographical distribution in annual precipitation changes

The geographical distribution of annual precipitation changes in three future time horizones with reference to base years is presented in Fig 10. A reduction of precipitation is noticed in the northwest of Iraq for all RCP. A higher decrease is projected in the northwest of Zones-I and II during 2010-2039 by -72 to -103 mm, while the highest increase in the central region and some parts in the northeast by approximately 9–20 mm for different RCPs. During 2040-2069, a decrease in precipitation is noticed in the northwest by -85 to -55 mm, while a higher increase in the central and east Iraq by 21–28 mm for different scenarios. The changes are found very similar during 2070-2099. The highest decrease are observed in Zone-III and northwest of Zone-II in the range of -94 to -58 mm, while the higher increase by around 6 to 24 mm at a few locations in the central, northeast and southeast of Iraq for different RCPs.

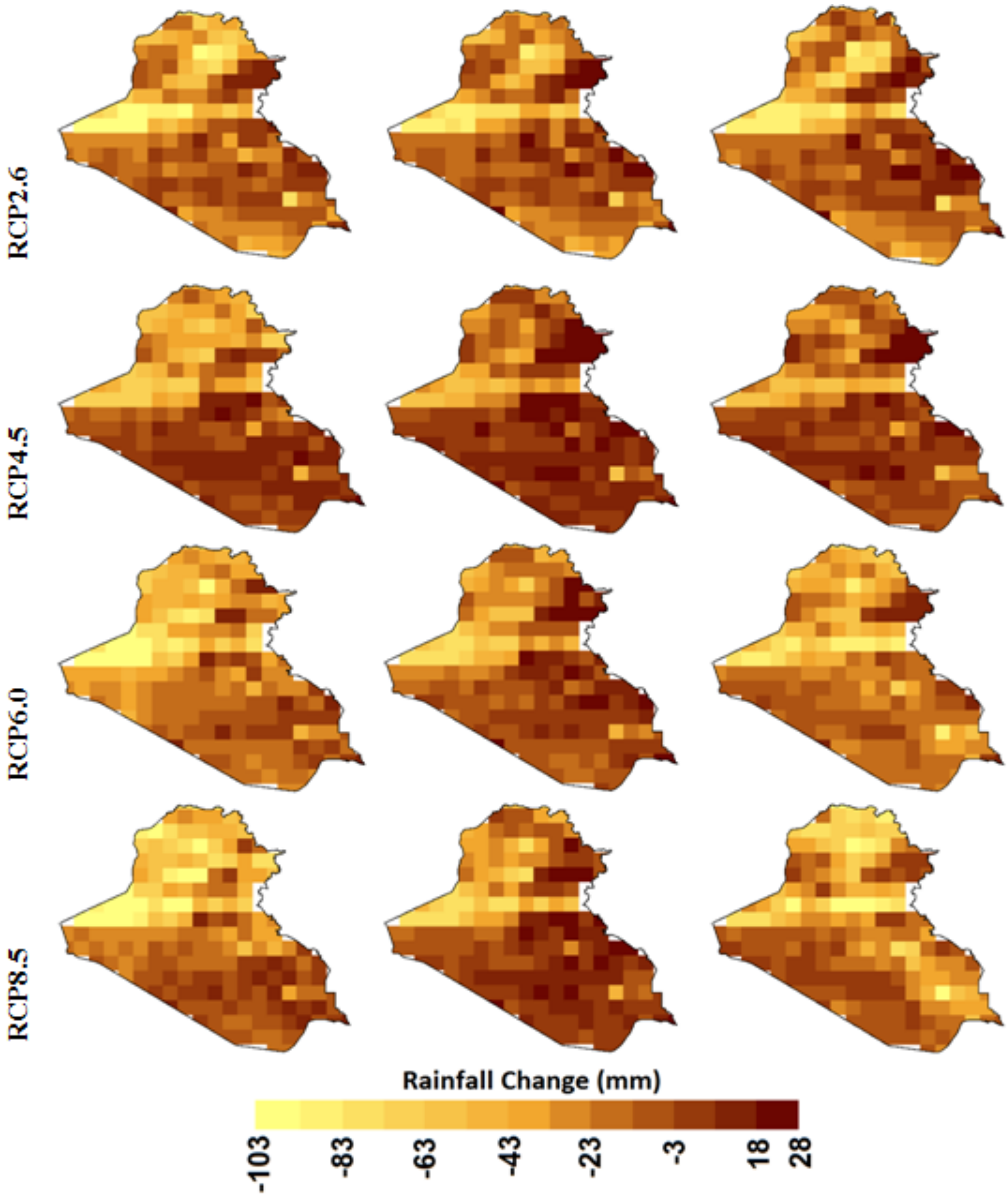

Fig 10. Geographical distribution of annual precipitation changes for three future periods and four RCPs.

4.7 Geographical distribution in seasonal precipitation changes

The geographical distributions of winter, autumn and spring precipitation changes for three future time horizones are presented in Figs 11, 12 and 13, respectively. The summer precipitation is very less; almost zero in most of the country. Changes in summer precipitation were also found very less and therefore, not presented here.

Fig 11 shows a reduction of winter precipitation in the north, while a slight augmentation in the southern region. The reduction of precipitation in the northern mountainous region is found up to 100 mm for RCP8.5 during 2070–2099. The increased precipitation in the southwestern desert is observed up to 15 mm for almost all scenarios.

Opposite scenarios are observed for spring. Increased precipitation is projected in the northern zone in the range of 7–13 mm, while a decrease in the northern part of the western desert up to -21 mm for most of the scenarios. Overall, the changes in precipitation in spring are found less. Precipitation projection for autumn is seen more or less similar to spring. Increased precipitation is projected in the north and a decrease in the west of Iraq. However, changes in autumn precipitation are found more compared to spring precipitation. An increase up to 23 mm in the north, while a decrease up to -30 mm in the north of the western desert are found for all RCPs.

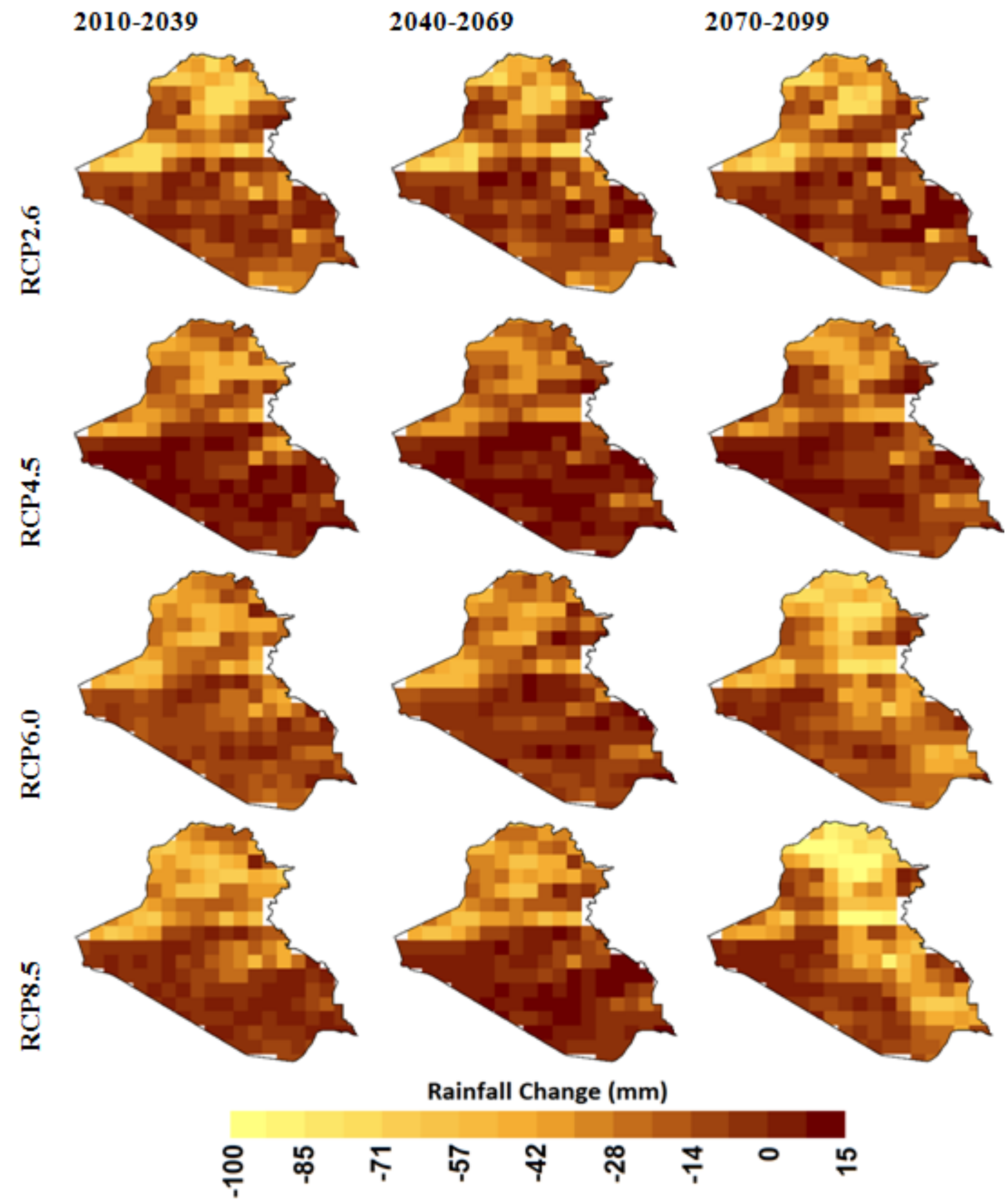

Fig 11. Geographical distribution of winter precipitation changes for three future periods and four RCPs

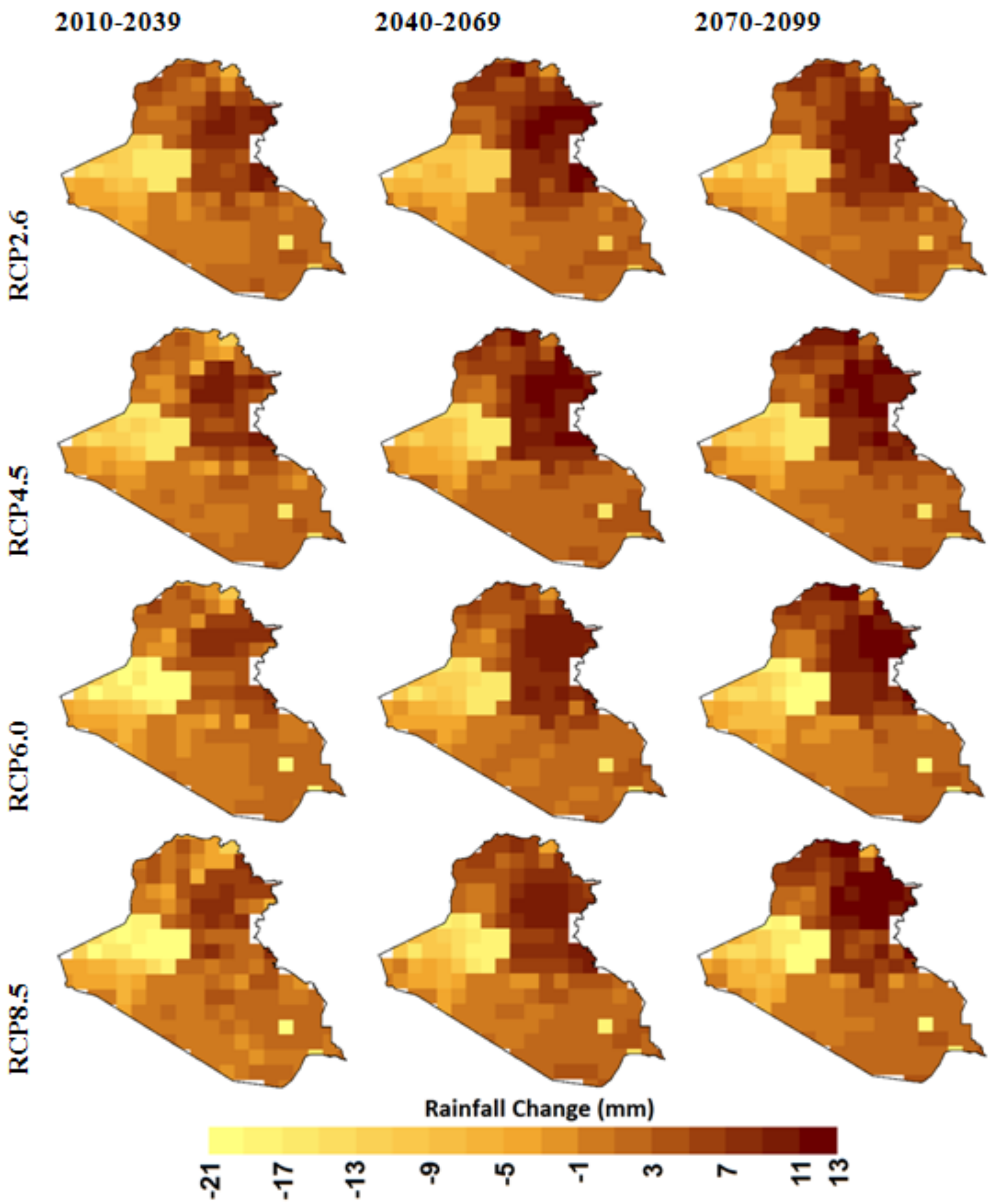

Fig 12. Geographical distribution of autumn precipitation changes for three future periods and four RCPs

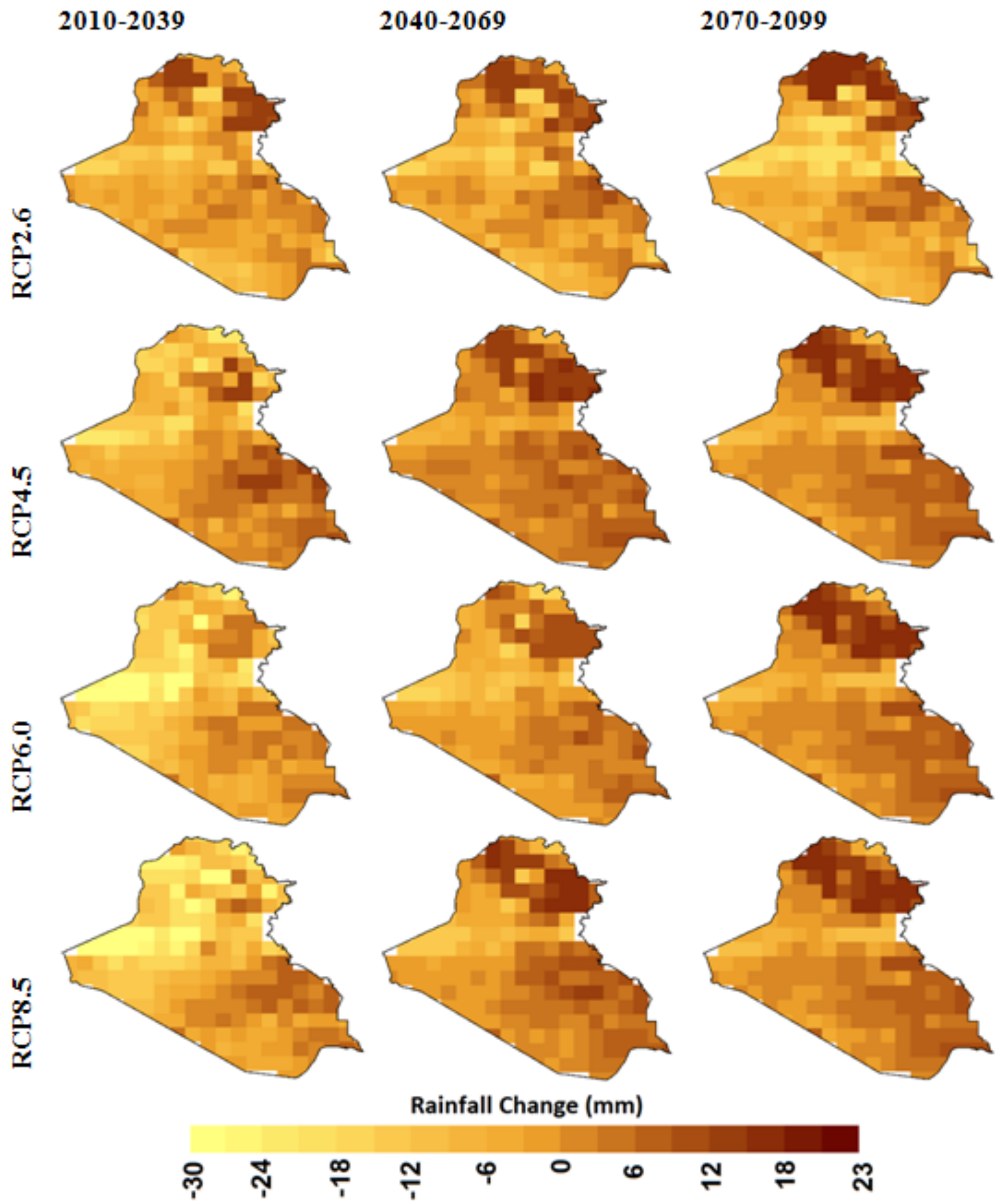

Fig 13. Geographical distribution of spring precipitation changes for three future periods and four RCPs.

Very limitted studies have assessed the possible changes in precipitation in the Arabian peninsula. Bozkurt and Sen (2013) projected climate in the Euphrates–Tigris Basin (ETB) using three GCMs for Special Report on Emissions Scenarios (SRES) scenarios and reported a possible abatement of winter precipitation in Zone-III and increase in the south of ETB. The study concluded that Iraq might experience more water stress due to reliance on the water supply of ETB on upstream countries. The findings correlate with the projections made in this study, which also reveals a significant reduction of winter precipitation in Zone-III and ian augmentation in the south of Iraq. Almazroui et al. (2016) used CMIP5 GCMs for projection in the Arabian Peninsula and reported precipitation reduction for RCP4.5 and RCP8.5 in southern Arabian Peninsula. The present study confirms a significant precipitation reduction over entire Iraq by 0% - 5% for all RCPs while a notable raise in the southern and west in a rate of 30 – 65% and at a rate of 20 -30% in the north of Iraq under most of RCPS. Peleg et al. (2015) employed four GCMs for precipitation projections over the Eastern Mediterranean region and projected less frequent precipitation (10–22% less) in the mid of this century. The present study also projects a possible reduction in precipitation in most of Iraq in all the seasons.

5. Conclusion

A methodology is proposed for the derivation of GCM ensemble and their downscaling for precipitation projections. Application of the proposed method selected two GCMs (HadGEM2-ES and HadGEM2-AO) for precipitation projection of Iraq. The results indicate that the SVM is capable to downscale GCM precipitation. The findings of the geographical distribution of precipitation changes estimated based on RF generated MME reveal a decrease in precipitation in the northwest of Iraq for all RCPs. The highest decrease during 2010-2039 is projected in the northwest of Zones-I and II, while an augmentation in the middle and some parts in the northeast of Iraq. The higher decrease in the precipitation in the middle of the century (2040-2069) is projected in the northwest, while an increase in the central and eastern Iraq. The changes are found very similar for the period 2070-2099. A large precipitation reduction is noticed in the north and northwest while an augmentation at a few locations in the central, northeast and southeast Iraq for the different RCPs. The precipitation projected with uncertainty estimated in the study can help policy-makers in streamlining the existing policies to improve climate resiliency. In future, multiple gridded precipitation datasets can be employed for the assessment of uncertainty in GCM selection and precipitation projections due to the gridded data used as a reference. Besides, other sophisticated ML methods can be applied for the implementation of downscaling model.

References

Ahmed K, Iqbal Z, Khan N, Rasheed B, Nawaz N, Malik I, Noor M (2019a) Quantitative assessment of precipitation changes under CMIP5 RCP scenarios over the northern sub-Himalayan region of Pakistan Environment, Development and Sustainability doi:10.1007/s10668-019-00548-5

Ahmed K, Sachindra D, Shahid S, Iqbal Z, Nawaz N, Khan N (2019b) Multi-model ensemble predictions of precipitation and temperature using machine learning algorithms Atmos Res:104806

Ahmed K, Sachindra DA, Shahid S, Demirel MC, Chung E-S (2019c) Selection of multi-model ensemble of general circulation models for the simulation of precipitation and maximum and minimum temperature based on spatial assessment metrics Hydrol Earth Syst Sci 23:4803-4824

Ahmed K, Shahid S, Haroon SB, Xiao-Jun W (2015) Multilayer perceptron neural network for downscaling rainfall in arid region: A case study of Baluchistan, Pakistan J Earth Syst Sci 124:1325-1341

Ahmed K, Shahid S, Nawaz N, Khan N (2019d) Modeling climate change impacts on precipitation in arid regions of Pakistan: a non-local model output statistics downscaling approach Theor Appl Climatol 137:1347-1364 doi:10.1007/s00704-018-2672-5

Ahmed K, Shahid S, Sachindra DA, Nawaz N, Chung E-S (2019e) Fidelity assessment of general circulation model simulated precipitation and temperature over Pakistan using a feature selection method J Hydrol 573:281-298 doi:https://doi.org/10.1016/j.jhydrol.2019.03.092

Ahmed K, Shahid S, Wang X, Nawaz N, Khan N (2019f) Spatiotemporal changes in aridity of Pakistan during 1901–2016 Hydrol Earth Syst Sci 23:3081-3096 doi:10.5194/hess-23-3081-2019

Akhter MS, Shamseldin AY, Melville BW (2019) Comparison of dynamical and statistical rainfall downscaling of CMIP5 ensembles at a small urban catchment scale Stoch Environ Res Risk Assess 33:989-1012 doi:10.1007/s00477-019-01678-y

Al-Ansari N (2013) Management of water resources in Iraq: perspectives and prognoses Engineering 5:667-684

Alamgir M, Khan N, Shahid S, Yaseen ZM, Dewan A, Hassan Q, Rasheed B (2020) Evaluating severity–area–frequency (SAF) of seasonal droughts in Bangladesh under climate change scenarios Stoch Environ Res Risk Assess 34:447-464 doi:10.1007/s00477-020-01768-2

Almazroui M, Saeed F, Islam MN, Alkhalaf A (2016) Assessing the robustness and uncertainties of projected changes in temperature and precipitation in AR4 Global Climate Models over the Arabian Peninsula Atmos Res 182:163-175

Bozkurt D, Sen OL (2013) Climate change impacts in the Euphrates–Tigris Basin based on different model and scenario simulations J Hydrol 480:149-161 doi:https://doi.org/10.1016/j.jhydrol.2012.12.021

Buytaert W, Friesen J, Liebe J, Ludwig R (2012) Assessment and management of water resources in developing, semi-arid and arid regions Water Resour Manage 26:841-844

Chiew FHS, Teng J, Vaze J, Kirono DGC (2009) Influence of global climate model selection on runoff impact assessment J Hydrol 379:172-180 doi:https://doi.org/10.1016/j.jhydrol.2009.10.004

Eden JM, Widmann M, Grawe D, Rast S (2012) Skill, Correction, and Downscaling of GCM-Simulated Precipitation J Clim 25:3970-3984 doi:10.1175/jcli-d-11-00254.1

Eden JM, Widmann M, Maraun D, Vrac M (2014) Comparison of GCM-and RCM-simulated precipitation following stochastic postprocessing Journal of Geophysical Research: Atmospheres 119

Fallmann J, Wagner S, Emeis S (2017) High resolution climate projections to assess the future vulnerability of European urban areas to climatological extreme events Theor Appl Climatol 127:667-683 doi:10.1007/s00704-015-1658-9

Gebrechorkos SH, Hülsmann S, Bernhofer C (2019) Regional climate projections for impact assessment studies in East Africa Environmental Research Letters 14:044031 doi:10.1088/1748-9326/ab055a

Groisman PY, Karl TR, Easterling DR, Knight RW, Jamason PF, Hennessy KJ, Suppiah R, Page CM, Wibig J, Fortuniak K (1999) Changes in the probability of heavy precipitation: important indicators of climatic change Clim Change 42:243-283

Houmsi MR, Shiru MS, Nashwan MS, Ahmed K, Ziarh GF, Shahid S, Chung E-S, Kim S (2019) Spatial Shift of Aridity and Its Impact on Land Use of Syria Sustainability 11:7047

IPCC (2007) Climate change 2007-the physical science basis: Working group I contribution to the fourth assessment report of the IPCC vol 4. Cambridge University Press, Khan N, Shahid S, Ahmed K, Ismail T, Nawaz N, Son M (2018) Performance Assessment of General Circulation Model in Simulating Daily Precipitation and Temperature Using Multiple Gridded Datasets Water 10:1793

Khan N, Shahid S, Ismail Tb, Wang X-J (2019) Spatial distribution of unidirectional trends in temperature and temperature extremes in Pakistan Theor Appl Climatol 136:899-913 doi:10.1007/s00704-018-2520-7

Lutz AF, ter Maat HW, Biemans H, Shrestha AB, Wester P, Immerzeel WW (2016) Selecting representative climate models for climate change impact studies: an advanced envelope-based selection approach Int J Climatol 36:3988-4005

McSweeney C, Jones R, Lee R, Rowell D (2015) Selecting CMIP5 GCMs for downscaling over multiple regions Clim Dyn 44:3237-3260

Moghim S, Bras RL (2017) Bias Correction of Climate Modeled Temperature and Precipitation Using Artificial Neural Networks J Hydrometeorol 18:1867-1884

Nashwan MS, Shahid S (2018) Spatial distribution of unidirectional trends in climate and weather extremes in Nile river basin Theor Appl Climatol:1-19

Nashwan MS, Shahid S, Abd Rahim N (2019) Unidirectional trends in annual and seasonal climate and extremes in Egypt Theor Appl Climatol 136:457-473 doi:10.1007/s00704-018-2498-1

Nashwan MS, Shahid S, Chung E-S (2020) High-Resolution Climate Projections for a Densely Populated Mediterranean Region Sustainability 12:3684

Navarro-Racines C, Tarapues J, Thornton P, Jarvis A, Ramirez-Villegas J (2020) High-resolution and bias-corrected CMIP5 projections for climate change impact assessments Scientific Data 7:7 doi:10.1038/s41597-019-0343-8

Noor M, bin Ismail T, Ullah S, Iqbal Z, Nawaz N, Ahmed K (2019a) A non-local model output statistics approach for the downscaling of CMIP5 GCMs for the projection of rainfall in Peninsular Malaysia Journal of Water and Climate Change

Noor M, Ismail Tb, Shahid S, Ahmed K, Chung E-S, Nawaz N (2019b) Selection of CMIP5 multi-model ensemble for the projection of spatial and temporal variability of rainfall in peninsular Malaysia Theor Appl Climatol doi:10.1007/s00704-019-02874-0

Onyutha C, Tabari H, Rutkowska A, Nyeko-Ogiramoi P, Willems P (2016) Comparison of different statistical downscaling methods for climate change rainfall projections over the Lake Victoria basin considering CMIP3 and CMIP5 Journal of hydro-environment research 12:31-45

Ouyang F, Zhu Y, Fu G, Lü H, Zhang A, Yu Z, Chen X (2015) Impacts of climate change under CMIP5 RCP scenarios on streamflow in the Huangnizhuang catchment Stoch Environ Res Risk Assess 29:1781-1795 doi:10.1007/s00477-014-1018-9

Peleg N, Bartov M, Morin E (2015) CMIP5-predicted climate shifts over the East Mediterranean: implications for the transition region between Mediterranean and semi-arid climates Int J Climatol 35:2144-2153 doi:10.1002/joc.4114

Pour SH, Harun SB, Shahid S (2014) Genetic programming for the downscaling of extreme rainfall events on the East Coast of Peninsular Malaysia Atmosphere 5:914-936

Pour SH, Shahid S, Chung E-S, Wang X-J (2018) Model output statistics downscaling using support vector machine for the projection of spatial and temporal changes in rainfall of Bangladesh Atmos Res 213:149-162 doi:https://doi.org/10.1016/j.atmosres.2018.06.006

Pour SH, Wahab AKA, Shahid S (2020) Spatiotemporal changes in aridity and the shift of drylands in Iran Atmos Res 233:104704

Press WH, Teukolsky SA, Vetterling WT, Flannery BP (1996) Numerical recipes in C vol 2. Cambridge university press Cambridge,

Sa'adi Z, Shahid S, Chung E-S, bin Ismail T (2017) Projection of spatial and temporal changes of rainfall in Sarawak of Borneo Island using statistical downscaling of CMIP5 models Atmos Res 197:446-460

Salman SA, Shahid S, Afan HA, Shiru MS, Al-Ansari N, Yaseen ZM (2020) Changes in Climatic Water Availability and Crop Water Demand for Iraq Region Sustainability 12:3437

Salman SA, Shahid S, Ismail T, Ahmed K, Chung E-S, Wang X-J (2019) Characteristics of Annual and Seasonal Trends of Rainfall and Temperature in Iraq Asia-Pacific Journal of Atmospheric Sciences doi:10.1007/s13143-018-0073-4

Salman SA, Shahid S, Ismail T, Ahmed K, Wang X-J (2018a) Selection of climate models for projection of spatiotemporal changes in temperature of Iraq with uncertainties Atmos Res 213:509-522 doi:https://doi.org/10.1016/j.atmosres.2018.07.008

Salman SA, Shahid S, Ismail T, Al-Abadi AM, Wang X-j, Chung E-S (2018b) Selection of gridded precipitation data for Iraq using compromise programming Measurement 132:87-98

Salman SA, Shahid S, Ismail T, Chung E-S, Al-Abadi AM (2017) Long-term trends in daily temperature extremes in Iraq Atmos Res 198:97-107

Salman SA, Shahid S, Ismail T, Rahman NbA, Wang X, Chung E-S (2018c) Unidirectional trends in daily rainfall extremes of Iraq Theor Appl Climatol 134:1165-1177 doi:10.1007/s00704-017-2336-x

Sarr B (2012) Present and future climate change in the semi-arid region of West Africa: a crucial input for practical adaptation in agriculture Atmos Sci Lett 13:108-112

Shahid S (2011) Trends in extreme rainfall events of Bangladesh Theor Appl Climatol 104:489-499 doi:10.1007/s00704-010-0363-y

Shahid S, Wang X-J, Harun SB, Shamsudin SB, Ismail T, Minhans A (2016) Climate variability and changes in the major cities of Bangladesh: observations, possible impacts and adaptation Regional environmental change 16:459-471

Shiru MS, Shahid S, Chung E-S, Alias N, Scherer L (2019a) A MCDM-based framework for selection of general circulation models and projection of spatio-temporal rainfall changes: A case study of Nigeria Atmos Res 225:1-16 doi:https://doi.org/10.1016/j.atmosres.2019.03.033

Shiru MS, Shahid S, Shiru S, Chung ES, Alias N, Ahmed K, Dioha EC, Sa'adi Z, Salman S, Noor M (2019b) Challenges in water resources of Lagos mega city of Nigeria in the context of climate change Journal of Water and Climate Change

Shirvani A, Landman WA (2016) Seasonal precipitation forecast skill over Iran Int J Climatol 36:1887-1900 doi:doi:10.1002/joc.4467

Shreem SS, Abdullah S, Nazri MZA (2016) Hybrid feature selection algorithm using symmetrical uncertainty and a harmony search algorithm International Journal of Systems Science 47:1312-1329

Turco M, Llasat MC, Herrera S, Gutiérrez JM (2017) Bias correction and downscaling of future RCM precipitation projections using a MOS-Analog technique Journal of Geophysical Research: Atmospheres 122:2631-2648

Vandal T, Kodra E, Ganguly AR (2019) Intercomparison of machine learning methods for statistical downscaling: the case of daily and extreme precipitation Theor Appl Climatol 137:557-570 doi:10.1007/s00704-018-2613-3

Wang X, Yang T, Li X, Shi P, Zhou X (2016) Spatio-temporal changes of precipitation and temperature over the Pearl River basin based on CMIP5 multi-model ensemble Stoch Environ Res Risk Assess:1-13

Wu Z, Chen X, Lu G, Xiao H, He H, Zhang J (2016) Regional response of runoff in CMIP5 multi-model climate projections of Jiangsu Province, China Stoch Environ Res Risk Assess 31:2627-2643

Xu K, Wu C, Hu BX (2019) Projected changes of temperature extremes over nine major basins in China based on the CMIP5 multimodel ensembles Stoch Environ Res Risk Assess 33:321-339 doi:10.1007/s00477-018-1569-2

Xu R, Chen N, Chen Y, Chen Z (2020) Downscaling and Projection of Multi-CMIP5 Precipitation Using Machine Learning Methods in the Upper Han River Basin Advances in Meteorology 2020

Yaseen ZM, Awadh SM, Sharafati A, Shahid S (2018) Complementary data-intelligence model for river flow simulation J Hydrol 567:180-190